Two Growth Modes of Metal Oxide in the Colloidal Crystal Template Leading to the Formation of Two Different Macroporous Materials

Xun Li, Yuan Jiang, Zhiwei Shi, and Zheng Xu*

State Key Laboratory of Coordination Chemistry and Laboratory of Solid State Microstructure, School of Chemistry and Chemical Engineering, Nanjing University, Jiangsu, People's Republic of China

Received May 1, 2007. Revised Manuscript Received August 22, 2007

The experimental results show that there are two growth modes of crystalline metal oxide in the colloidal crystal template, which depend on the quality of the colloidal crystal. In well-ordered colloidal crystal templates, the metal oxide growth follows the structure of the colloidal crystal; and high quality three-dimensional ordered macroporous (3DOM) Cu_2O or ZnO are formed. In contrast, in less-ordered colloidal crystal templates, metal oxide is grown according to its own capital structure, and cubic-shaped macroporous Cu_2O or sheetlike macroporous ZnO are formed. Our method provides an easy and convenient way to prepare three-dimensional ordered macroporous materials or shaped macroporous materials via adjusting the level of ordered arrangement of the colloidal crystal templates.

Introduction

Recently, three-dimensional ordered macroporous (3DOM) materials have attracted intensive interest. Their unique properties, such as uniform submicrometer scale pore sizes, highly ordered pore structure, and large accessible surface, make them suitable for applications in photonic band gap crystals,[1,2] battery electrodes,[3,4] and gas sensors.[5,6] Despite the fact that various fabrication methods have been developed, the method using colloidal crystals as templates is simple and efficient. In this method, the key step is the construction of close-packed colloidal crystals. 3DOM materials are fabricated only with high-quality colloidal crystals as templates.[7−9] However, without careful control, colloidal crystals with defects or disordered arrangement are easily formed. The interest here focuses on the question of what happens when less-ordered colloidal crystals are used as templates.

Many scientists paid a lot of attention to 3DOM materials in the past decade, but the construction of shaped macroporous materials was neglected. Only a few reports focused on the fabrication of shaped macroporous materials,[10−14] let alone the controllable fabrication of shaped macroporous and 3DOM materials. Recently, Lu et al. synthesized octahedral Cu_2O−P(St−MMA−AA) composite particles by using copolymer latex particles as templates, and pores formed only on the surface.[10] Liu et al. obtained porous ZnO nanosheets by electrochemical deposition, with polystyrene (PS) colloidal crystals as templates.[13] Fu et al. deposited $Zn(NO_3)(OH)\cdot H_2O$ into the interstices of a colloidal crystal array. After the PS spheres were removed, $Zn(NO_3)(OH)\cdot H_2O$ was converted to ZnO by calcination and porous ZnO nanosheets were obtained.[14] In another experiment, the group used zinc as a precursor to prepare the ZnO inverse opal using the multipotential step method. As far as anyone knows, no effective methods have been reported that can achieve selective formation of shaped macroporous and 3DOM materials. Therefore, there is an urgent need to develop a facile and controllable fabrication method for shaped macroporous and 3DOM materials.

In our previous work, 3DOM Cu_2O was obtained, as well as some multitriangular Cu_2O was formed in a few defective areas.[15] After that, we got interested in the forming mechanism of these shaped macroporous materials. Here, we report a facile way for controllable fabrication of shaped macroporous and 3DOM Cu_2O (ZnO), respectively. The

* Corresponding author. E-mail: zhengxu@netra.nju.edu.cn. Tel.:+86-25-83593133. Fax: +86-25-83314502.

(1) Vlasov, Y. A.; Bo, X. Z.; Sturm, J. C.; Norris, D. J. *Nature* **2001**, *414*, 289−293.
(2) Müller, M.; Zentel, R.; Maka, T.; Romanov, S. G.; Torres, C. M. S. *Adv. Mater.* **2000**, *12*, 1499−1503.
(3) Lee, K. T.; Lytle, J. C.; Ergang, N. S.; Oh, S. M.; Stein, A. *Adv. Funct. Mater.* **2005**, *15*, 547−556.
(4) Mihi, A.; Míguez, H. *J. Phys. Chem. B* **2005**, *109*, 15968−15976.
(5) Scott, R. W. J.; Yang, S. M.; Chabanis, G.; Coombs, N.; Williams, D. E.; Ozin, G. A. *Adv. Mater.* **2001**, *13*, 1468−1472.
(6) Acciarri, M.; Barberini, R.; Canevali, C.; Mattoni, M.; Mari, C. M.; Morazzoni, F.; Nodari, L.; Polizzi, S.; Ruffo, R.; Russo, U.; Sala, M.; Scotti, R. *Chem. Mater.* **2005**, *17*, 6167−6171.
(7) McLachlan, M. A.; Johnson, N. P.; De La Rue, R. M.; McComb, D. W. *J. Mater. Chem.* **2004**, *14*, 144−150.
(8) Li, H. L.; Marlow, F. *Chem. Mater.* **2006**, *18*, 1803−1810.
(9) Ye, Y. H.; LeBlanc, F.; Haché, A.; Truong, V. V. *Appl. Phys. Lett.* **2001**, *78*, 52−54.
(10) Lu, C.; Qi, L.; Cong, H.; Wang, X.; Yang, J.; Yang, L.; Zhang, D.; Ma, J.; Cao, W. *Chem. Mater.* **2005**, *17*, 5218−5224.
(11) Xu, L.; Zhou, W. L.; Frommen, C.; Baughman, R. H.; Zakhidov, A. A.; Malkinski, L.; Wang, J. Q.; Wiley, J. B. *Chem. Commun.* **2000**, 997−998.
(12) Bartlett, P. N.; Dunford, T.; Ghanem, M. A. *J. Mater. Chem.* **2002**, *12*, 3130−3135.
(13) Liu, Z.; Jin, Z.; Li, W.; Liu, X.; Qiu, J.; Wu, W. *Mater. Lett.* **2006**, *60*, 810−814.
(14) Fu, M.; Zhou, J.; Xiao, Q.; Li, B.; Zong, R.; Chen, W.; Zhang, J. *Adv. Mater.* **2006**, *18*, 1001−1004.
(15) Li, X.; Tao, F.; Jiang, Y.; Xu, Z. *J. Colloid Interface Sci.* **2007**, *308*, 460−465.

10.1021/cm071180f CCC: $37.00
Published on Web 10/06/2007

experiment results show that there are two types of growth modes: one forms a large area of close-packed 3DOM Cu_2O (ZnO), using the well-ordered colloidal crystals as templates; the other generates cubic-shaped macroporous Cu_2O or sheetlike macroporous ZnO out of the less-ordered colloidal crystal templates. To the very best of our knowledge, this is the first report about the controllable fabrication of shaped macroporous and 3DOM materials by simply adjusting the order level of the colloidal crystals.

Experimental Section

Materials. Styrene (C.P.), potassium persulfate (A.R.), ethanol (A.R.), acetone (A.R.), cupric sulfate pentahydrate (A.R.), lactic acid (A.R.), zinc nitrate hexahydrate (A.R.), sodium hydroxide (A.R.), tetrahydrofuran (THF) (A.R.), and glass slides coated with indium−tin oxide (ITO) ($R_s = 30\ \Omega$) are all commercially available products. Styrene was washed three times with 10 wt % NaOH solution, followed by another three times with deionized water before use. ITO/glass was washed by acetone, ethanol, and deionized water, respectively, under sonication before use. Other materials were used without further purification.

Fabrication of PS Colloidal Crystal Templates. PS microspheres with diameters of about 350 nm were synthesized by the surfactant-free emulsion polymerization method.[16] In brief, an aqueous emulsion composed by 60 wt % ethanol, 34.9 wt % deionized water, 5 wt % styrene, and 0.1 wt % potassium persulfate was polymerized at 70 °C for 24 h under nitrogen atmosphere. Then, the latex particles were washed with deionized water three times by centrifugation and filtration to remove the unreacted styrene and inorganic product. The well-ordered colloidal crystal templates were assembled on ITO glass substrate which is submerged vertically into an aqueous dispersion of PS spheres (0.8 wt %) at 65 °C.[7] The process ended when the volume of the aqueous suspension solution reduced to one-fourth of the initial volume. Meanwhile, the less-ordered colloidal crystal templates were assembled in an ethanol dispersion of PS spheres at 65 °C under the same procedure. After being dried at room temperature, both of the colloidal crystal templates were heated at 100 °C for 10 min to increase the structural stability.

Fabrication of Cu_2O Macroporous Materials. The Cu_2O macroporous materials were constructed by electrochemical reduction of copper(II) lactate in alkaline solution.[17] The electrolyte solution was composed of 0.4 M $CuSO_4$ and 3 M lactic acid; the pH value of the solution was adjusted to 12 by 10 wt % NaOH solution. Cu_2O was grown potentiostatically in a three-electrode system controlled by an EG&G PAR 273A potentiostat. ITO substrate covered with colloidal crystals was used as the working electrode; a copper wire and a saturated calomel reference electrode (SCE) were used as the counter electrode and reference electrode, respectively. The potentiostatic deposition was performed at −0.5 V versus SCE for a given time, and the deposition temperature was kept constant at 45 °C. The macroporous Cu_2O was obtained after PS was removed in THF. As a comparison, the pore-free Cu_2O was electrodeposited on the bare ITO substrate by the same method.

Fabrication of ZnO Macroporous Materials. ZnO was electrodeposited in 0.10 M $Zn(NO_3)_2$ aqueous solution.[18] ZnO was grown potentiostatically in a three-electrode system controlled by an EG&G PAR 273A potentiostat. ITO glass substrate covered with colloidal crystals was used as the working electrode with a platinum plate counter electrode and an SCE reference electrode. The potentiostatic deposition was performed at −0.95 V versus SCE for 10 min, and the deposition temperature was kept constant at 60 °C. The macroporous ZnO was obtained after the PS was removed in THF. As a comparison, the pore-free ZnO was electrodeposited on the bare ITO substrates by the same method.

Characterization. The morphologies of macroporous and pore-free materials were imaged with a JEOL JEM-5610LV scanning electron microscope (SEM) at 15 kV. Transmission electron microscopy (TEM) images and selected area electron diffraction (SAED) patterns were obtained on a JEOL JEM-200CX transmission electron microscope at 160 kV. The phase structures were characterized by power X-ray diffractometry (SHIMADZU XRD-6000 X-ray diffractometer with graphite-monochromatized Cu Kα radiation, $\lambda = 0.15406$ nm). The near-infrared transmission spectra of PS colloidal crystal templates were recorded by a Shimadzu UV-3100 UV−vis−near-infrared spectrophotometer.

Results and Discussion

Well-Ordered and Less-Ordered PS Colloidal Crystal Templates. As shown in Figure 1, parts a and b, well-ordered and less-ordered colloidal crystal templates were assembled in the aqueous and ethanol dispersion of PS spheres, respectively. As the evaporation speed of ethanol is faster than that of water at the same temperature, the PS spheres in the ethanol suspension sedimentated faster and did not have enough time to move into the right lattice sites. Meanwhile, the faster evaporation of ethanol resulted in intense convection to disturb the arrangement of the PS spheres. These two factors led to the formation of the less-ordered PS colloidal crystal templates in the ethanol system. Figure 1a shows a typical SEM image of the well-ordered PS colloidal crystal templates. In these templates, the hexagonally packed layers of the (111) face of the face-centered cubic (fcc) lattice are demonstrated with few defects. In the less-ordered colloidal crystal templates shown in Figure 1b, there are vacancies as well as cracks and plane stacking defects. In an even larger area of ∼50 μm × 60 μm, the ordered packed area usually extends to hundreds of square-micrometers in the well-ordered colloidal crystal templates (see the Supporting Information, Figure S1a), whereas the ordered packed areas are always as small as several square-micrometers in the less-ordered colloidal crystal templates (see the Supporting Information, Figure S1b). But it must be mentioned that the less-ordered templates used here are not homogeneously poor-ordered; there are still many small blocks which are order-packed. The quality of the colloidal crystal can be represented by a transmission spectra because the presence of defects results in the appearance of strongly localized photonic bandtail states and thus enhances the transmission in the gap.[9] Although the thickness of the template affects the depth of the photonic stop band gap,[19] the thickness of the well-ordered and less-ordered colloidal crystal templates which were assembled from the colloidal suspensions with the same concentration are almost the same. Thus, the main effect here

(16) Homola, A. M.; Inoue, M.; Robertson, A. A. *J. Appl. Polym. Sci.* **1975**, *19*, 3077−3086.
(17) Golden, T. D.; Shumsky, M. G.; Zhou, Y.; VanderWerf, R. A.; Van Leeuwen, R. A.; Switzer, J. A. *Chem. Mater.* **1996**, *8*, 2499−2504.
(18) Yoshida, T.; Tochimoto, M.; Schlettwein, D.; Oekermann, T.; Sugiura, T.; Minoura, H. *Chem. Mater.* **1999**, *11*, 2657−2667.
(19) Im, S. H.; Kim, M. H.; Park, O. O. *Chem. Mater.* **2003**, *15*, 1797−1802.

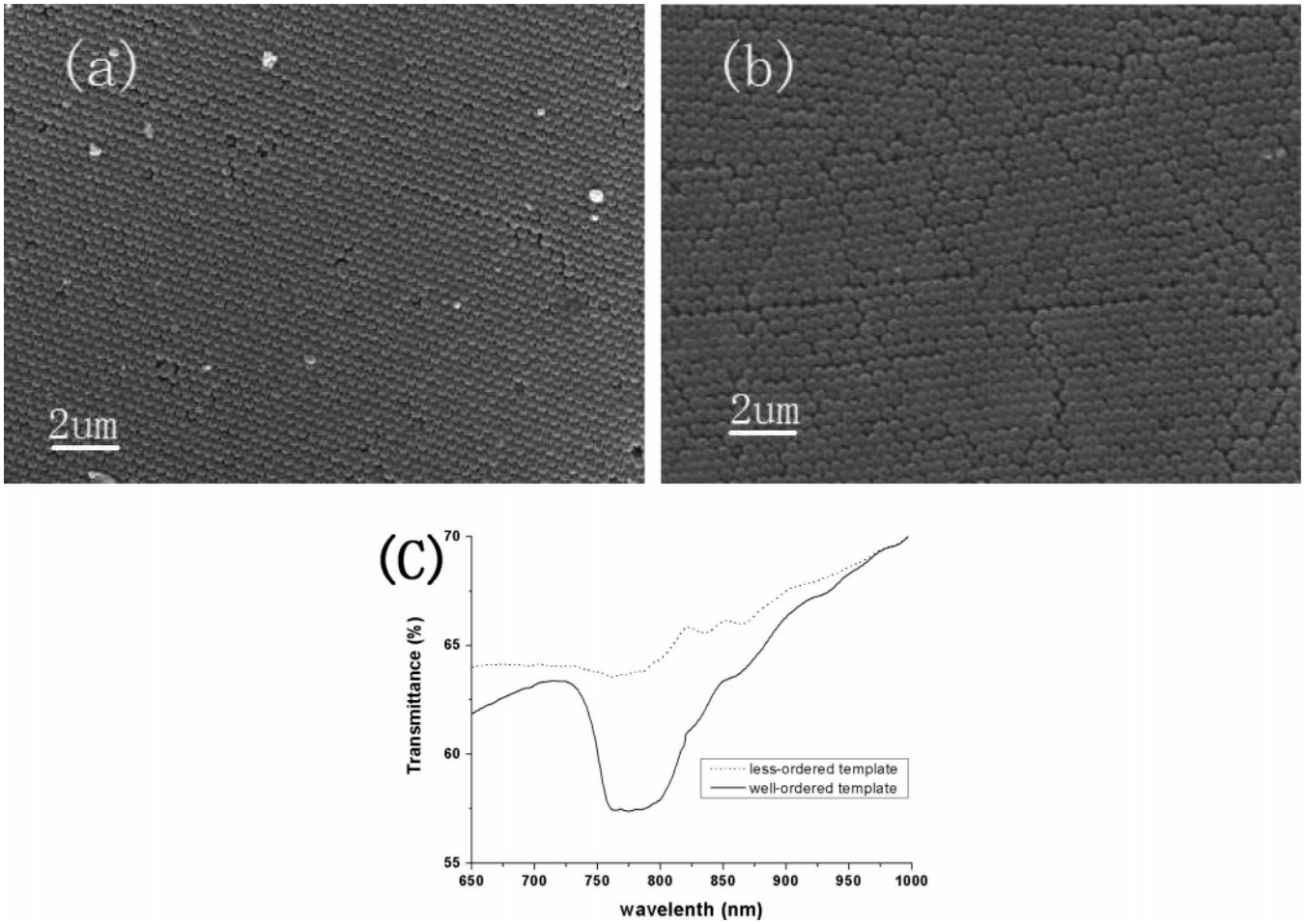

Figure 1. SEM images of (a) well-ordered PS colloidal crystal templates; (b) less-ordered PS colloidal crystal templates. (c) Transmission spectra at normal incidence for both well-ordered and less-ordered colloidal crystal templates.

is the colloidal crystalline quality. Figure 1c shows the transmission spectra measured at a normal incidence for these two templates. A pronounced attenuation dip in transmission around 785 nm can be observed in the well-ordered colloidal crystal template, whereas a shallow attenuation in transmission can be found in the less-ordered one. The transmission in the gap increases, resulting from an increase of disorder arrangement in the template. It is easy to find that the crystalline quality is higher in the well-ordered template than that in the less-ordered one, which fits well with the SEM results. The small decrease in transmission, around 785 nm, in the less-ordered colloidal crystal template is attributed to many small ordered packed blocks in it.

Cubic Macroporous Cu_2O Materials. In a controlled experiment, pore-free Cu_2O cubes were obtained on the bare ITO substrate by electrodeposition (Figure 2, parts a and b), which was similar to the previous reports[17,20] and indicated that Cu_2O intended to form cubes in these experiment conditions. When the less-ordered colloidal crystals were used as templates, cubic-shaped macroporous Cu_2O materials were obtained by electrodeposition for 3 min after the PS spheres were removed (Figure 2, parts c and d). The less-ordered porous structure in the cube mirrored the fact that PS spheres formed a less-ordered array in the template, as shown in Figure 1b. The cubic shape of the macroporous Cu_2O was the same as that of the pore-free one, which meant the less-ordered templates had little spatial confined effect on the growth of Cu_2O, and the growth of the cubic-shaped Cu_2O followed its own capital structure. When the electrodeposition time reduced to 90 s, using the less-ordered colloidal crystal templates, only a small amount of small porous cubes were spread on the ITO substrates (Figure 2e). In spite of the defects, there were still some short-range ordered packed areas within several square-micrometers in the less-ordered colloidal crystal templates, as shown in Figure 1b. Therefore, it was concluded that Cu_2O was initially grown from the defects of the colloidal crystal on the ITO substrate, where the infiltration of the electrolyte solution was easier. As the defects were surrounded by the ordered packed area, the electrolyte solution did not have enough time to infiltrate. In this case, blanks were left after the ordered packed PS spheres were removed, and the porous cubes were dispersed on the ITO substrate. The magnified SEM image of these small porous cubes showed that many of them were only three layers with pores throughout the bottom (Figure 2f). With longer electrodeposition time, the small porous cubes could be grown much larger. From Figure 2d, one can easily see that the larger porous cubes were grown from the smaller ones. Thus, pores going through the larger cubes were expected.

(20) Liu, R.; Oba, F.; Bohannan, E. W.; Ernst, F.; Switzer, J. A. *Chem. Mater.* **2003**, *15*, 4882−4885.

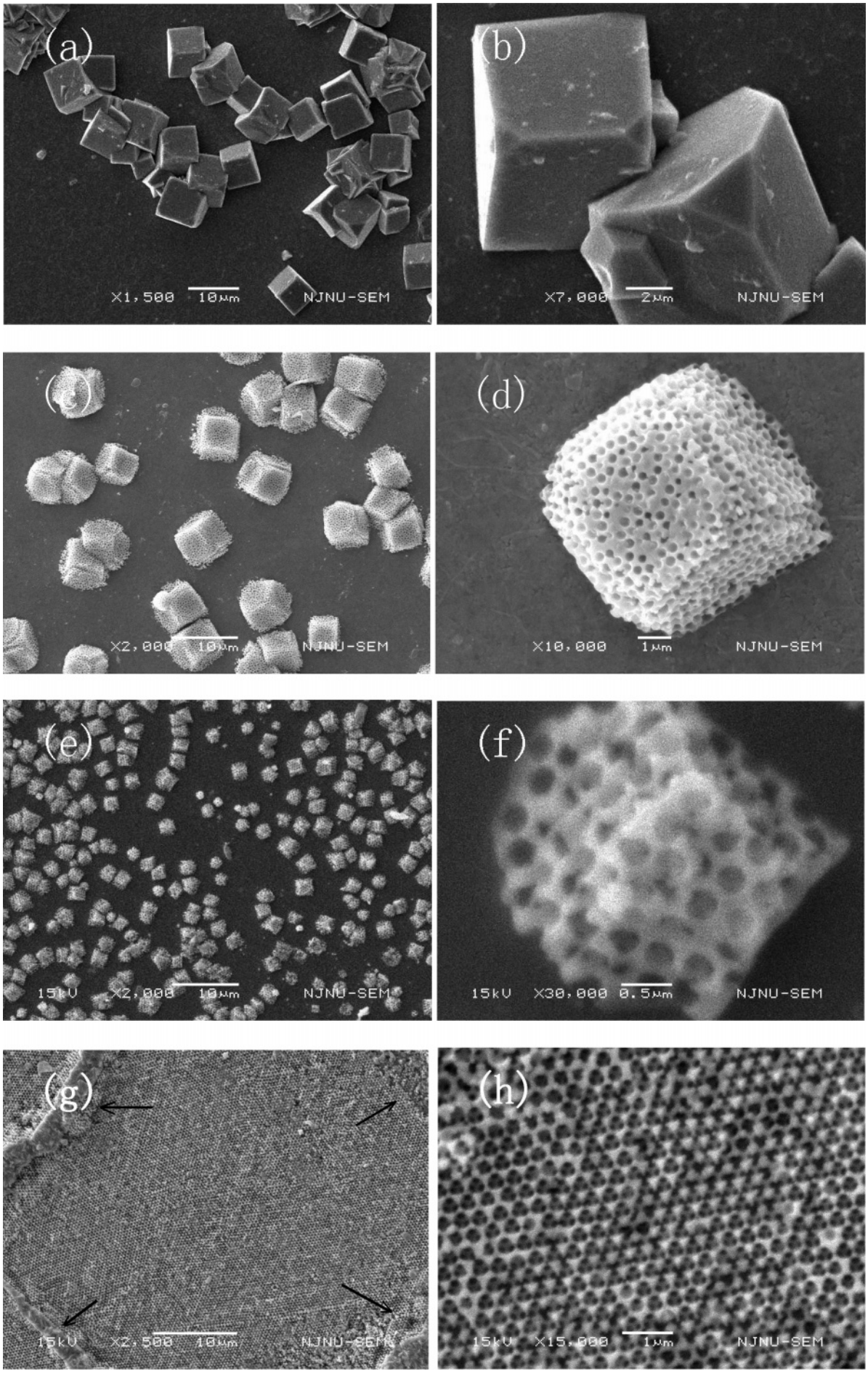
(a)
X1,500 10μm NJNU-SEM
(b)
X7,000 2μm NJNU-SEM
(c)
X2,000 10μm NJNU-SEM
(d)
X10,000 1μm NJNU-SEM
(e)
15kV X2,000 10μm NJNU-SEM
(f)
15kV X30,000 0.5μm NJNU-SEM
(g)
15kV X2,500 10μm NJNU-SEM
(h)
15kV X15,000 1μm NJNU-SEM

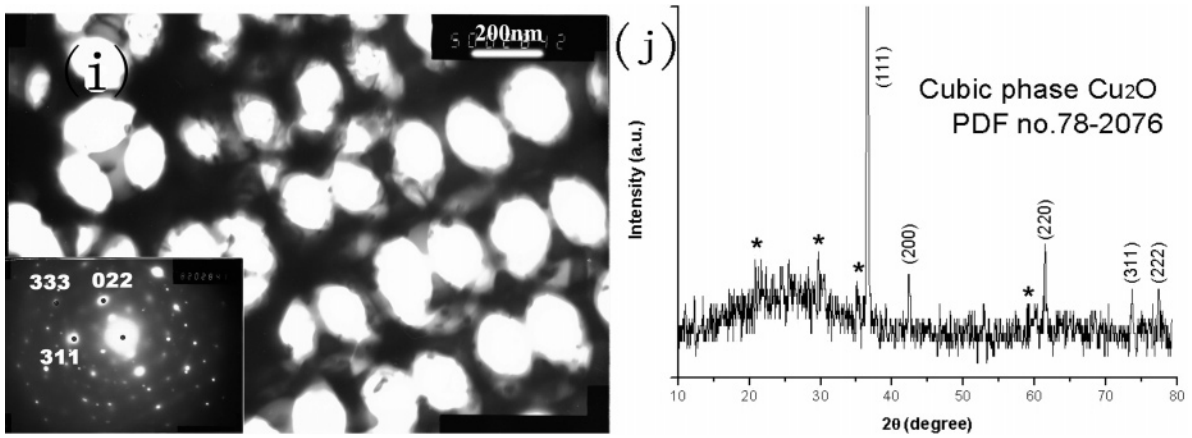

Figure 2. SEM images of (a) pore-free cubic Cu_2O electrodeposited for 3 min; cubic Cu_2O macroporous materials electrodeposited for (c) 3 min and (e) 90 s; (g) Cu_2O 3DOM materials electrodeposited for 10 min; (b), (d), (f), and (h) the magnification images of (a), (c), (e), and (g), respectively; (i) TEM image of electrodeposited Cu_2O 3DOM materials with SAED pattern inset; (j) powder XRD pattern of electrodeposited Cu_2O 3DOM materials. Peaks with an asterisk are attributed to the ITO substrate.

Morphology Evolution of the Cubic Macroporous Cu_2O Materials. Experimental results indicate that the morphology of shaped Cu_2O macroporous materials is closely related to the electrodeposition time. As shown in Figure 2a, the dispersed cubic-shaped Cu_2O particles were synthesized by electrodeposition in 3 min. Those Cu_2O cubes were believed to be grown directly from the defects of the colloidal crystals on the ITO substrate. When the electrodeposition time was extended to 5 min, more cubes were observed on the substrate (see the Supporting Information, Figure S2, parts a and c), although, when the electrodeposition lasted for more than 10 min, the cubes were found to be connected to each other and spread over the whole ITO substrate (see the Supporting Information, Figure S2, parts b and d). From Figure 2, parts a, c, e, and Figure S2, it could be conceived that the morphology evolution of shaped Cu_2O follows a similar way for both the template-free and less-ordered colloidal crystal templates. Thus, the less-ordered templates had little spatial confined effect on the growth of Cu_2O; Cu_2O crystals were grown into cubic shape as freely as on the bare substrate.

Three-Dimensional Ordered Macroporous Cu_2O Materials. When the well-ordered colloidal crystals were used as templates, 3DOM Cu_2O (Cu_2O inverse opals) were generated (Figure 2, parts g and h).[15] The pores were well-ordered in the fcc close-packed structure, which was consistent with the (111) plane arrangement of an fcc structure and copied the structure of the original colloidal crystal templates, as shown in Figure 1a. The Cu_2O could only be grown in the space between the well-ordered arranged PS spheres, where spatial confined effect played a critical role. In Figure 2, parts g and h, the top of the 3DOM Cu_2O material shows a smooth and flat plane. Evidently, Cu_2O was grown homogeneously in the template, because of the same diffusion rate of the reactants in each channel of the well-ordered structure. Therefore, the Cu_2O product copied the fcc structure of the colloidal crystal template to form a perfect close-packed macroporous material, after the PS spheres were removed. As shown in Figure 1a, even in the large area of well-ordered colloidal crystal templates, defects were inevitable. Because of better diffusion of reactants in the defects, Cu_2O was grown faster to form the ridge (marked with arrows in Figure 2g), which was similar to the connected cubes in Figure S2, parts b and d. When the well-ordered colloidal crystals were used as templates, the change in electrodeposition time only resulted in a change in the thickness, instead of the shape of the 3DOM Cu_2O materials. This difference provides further evidence that there exist two types of growth modes: in the well-ordered colloidal crystal templates, the colloidal crystal structure of the template plays a critical role, whereas in the less-ordered templates, the oxide capital structure itself acts as a key factor. Figure 2i shows a typical TEM image of a chip of macroporous Cu_2O from the 3DOM Cu_2O materials, which suggests that the pores are well-ordered and interconnected with small channels. The SAED pattern corresponding to the wall area shows that the electrochemically deposited Cu_2O is nearly single-crystalline. Although more than one set of diffraction spots were found, the clear spots can be indexed as (022), (311), and (333) Bragg reflections of the primitive cubic lattice with the cell parameters $a = 4.27$ Å, consistent with the XRD result (Figure 2j). XRD patterns provide evidence that the 3DOM Cu_2O material is a pure cubic phase Cu_2O, which is in good accordance with PDF no.78-2076. Peaks with an asterisk are attributed to the ITO substrate, and the broad amorphous peak between 15° and 38° belongs to the glass substrate. The internal crystallinity of the Cu_2O crystal kept the same in the same electrodeposition conditions,[17,20] thus resulting in similar SAED and XRD patterns of 3D ordered and cubic-shaped macroporous Cu_2O materials.

Three-Dimensional Ordered and Sheetlike Macroporous ZnO Materials. A similar phenomenon was found in the fabrication of ZnO macroporous materials. High preference was found in pore-free sheetlike ZnO obtained on bare ITO substrates as mentioned in previous reports.[18] Less-ordered colloidal crystal templates led to less-ordered macroporous sheetlike ZnO (Figure 3, parts c and d), which was similar to Liu et al.'s results.[13] On the other hand, well-ordered colloidal crystal templates brought well-ordered macroporous ZnO materials (Figure 3, parts e and f). The TEM image (Figure 3g) shows the macroporous structure of 3DOM ZnO,

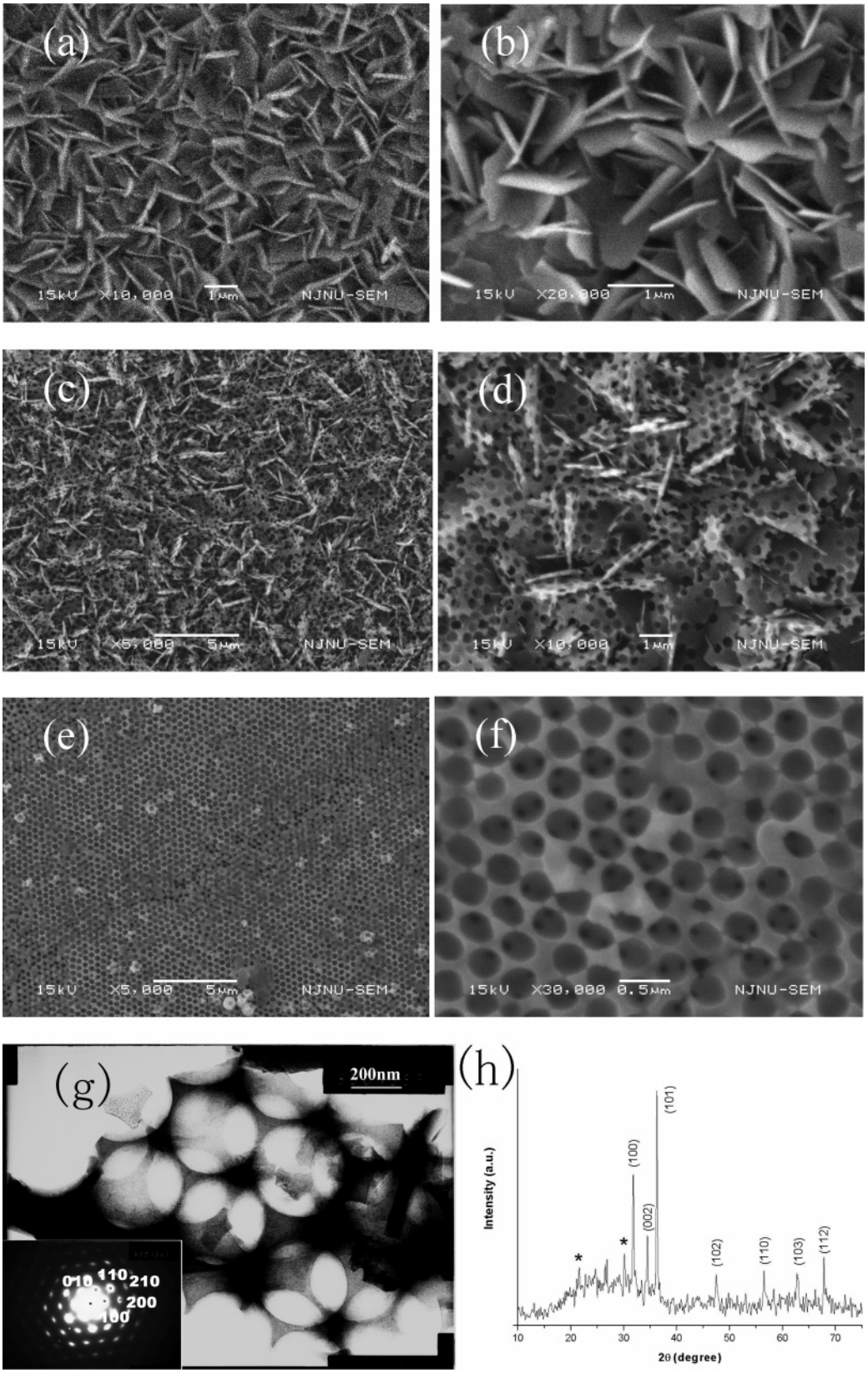

Figure 3. SEM images of (a) pore-free sheetlike ZnO; (c) sheetlike macroporous ZnO materials; (e) ZnO 3DOM materials; (b), (d), and (f) the magnification images of (a), (c), and (e), respectively; (g) TEM image of electrodeposited 3DOM ZnO with SAED pattern inset; (h) powder XRD pattern of electrodeposited 3DOM ZnO. Peaks with an asterisk are attributed to the ITO substrate.

and the hexagonal SAED pattern reveals that it is a perfect primitive hexagonal single crystal with $a = 3.25$ Å and $c = 5.21$ Å. XRD patterns (Figure 3h) also prove that pure ZnO obtained in these experimental conditions is in the hexagonal phase, which is in good accordance with PDF no.79-2205. This result gave a further confirmation to the assumption that there are two different growth modes in the well-ordered and less-ordered colloidal crystal templates, respectively. In

the same electrodeposition conditions, SAED and XRD patterns of 3D ordered and sheetlike macroporous ZnO materials are almost the same.[21]

Conclusions

Cu_2O and ZnO 3DOM materials, cubic-shaped Cu_2O, and sheetlike ZnO macroporous materials were successfully constructed through electrodeposition, by using PS colloidal crystals as templates. We demonstrated that the growth of these two crystalline oxides completely followed the template structure in the well-ordered colloidal crystal templates, because the electrolyte solution reached the ITO substrate via diffusing along the template channels at the same time and the growth rates of the crystalline oxide are the same along every channel. On the other hand, in the less-ordered templates, the diffusion rates of the electrolyte solution are different at different places and the growth rate of the crystalline oxide is faster in the defective area, which promotes the oxide growth following its own capital structure. To the very best of our knowledge, this is the first report about the controllable fabrication of shaped macroporous and 3DOM materials, and it may be extended to fabricate other metal oxides and sulfides.

Acknowledgment. The financial support by National Natural Science Foundation of China (NNSFC) under major project nos. 90606005, 20490210, 20571040, and 20371026 was gratefully acknowledged. We also thank Dr. Mintang Liu and Dr. Kirk Michael Mulligan (University of Saskatchewan, Canada) for some useful advice.

Supporting Information Available: Figures S1 and S2 (PDF). This material is available free of charge via the Internet at http://pubs.acs.org.

CM071180F

(21) Izaki, M.; Omi, T. *Appl. Phys. Lett.* **1996**, *68*, 2439−2440.